1,3,6,7-tetrahydroxy-8-prenylxanthone ameliorates inflammatory responses resulting from the paracrine interaction of adipocytes and macrophages

Running title: A xanthone abates adipose tissue inflammation

Dan Li[1], Qianyu Liu[1], Wen Sun[1], Xiuping Chen[1], Ying Wang[1], Yuxiang Sun[2], & Ligen Lin[1,*]

[1]State Key Laboratory of Quality Research in Chinese Medicine, Institute of Chinese Medical Sciences, University of Macau, Taipa, Macau, China and [2]Department of Nutrition and Food Science, Texas A&M University, College Station, TX, USA

[*]**Correspondence**

Ligen Lin, Institute of Chinese Medical Sciences, University of Macau, Avenida da Universidade, Taipa, Macau, China; Tel.: 853 88228041; fax: 853 28841358. E-mail: ligenl@umac.mo.

Table S1. Real-Time PCR primer sequences.

Gene	Forward	Reverse
18s	AGCCTGCGGCTTAATTTGAC	CAACTAAGAACGGCCATGCA
Arginase-1	CTCCAAGCCAAAGTCCTTAGAG	AGGAGCTGTCATTAGGGACATC
Ccl5	TGCAGAGGACTCTGAGACAGC	GAGTGGTGTCCGAGCCATA
Ccl11	AGAGCTCCACAGCGCTTCT	GCAGGAAGTTGGGATGGA
CD11c	CTGGATAGCCTTTCTTCTGCTG	GCACACTGTGTCCGAACTC
CD206	CAGGTGTGGGCTCAGGTAGT	TGTGGTGAGCTGAAAGGTGA
CD44	CCAGGCTTTCAACAGTACCTTACC	CTGAGGCATTGAAGCAATATGTGTC
CD68	CCTTATGGACAGCTTACCTTTGG	CTGAGCAGCCTGTAGCCTTAGAG
COX-2	CCACCTCTGCGATGCTCTTC	CATTCCCCACGGTTTTGACATG
Cx3cl1	CATCCGCTATCAGCTAAACCA	CAGAAGCGTCTGTGCTGTGT
Cxcl10	GCTGCCGTCATTTTCTGC	TCTCACTGGCCCGTCATC
F4/80	CTTTGGCTATGGGCTTCCAGTC	GCAAGGAGGACAGAGTTTATCGTG
IFN-γ	GTCATTGAAAGCCTAGAAAGTCTGA	CTGTGGGTTGTTGACCTCAAACT
IL-1β	TGTTCTTTGAAGTTGACGGACCC	TCATCTCGGAGCCTGTAGTGC
IL- 6	CCAGAGATACAAAGAAATGATGG	ACTCCAGAAGACCAGAGGAAAT
iNOS	CCAAGCCCTCACCTACTTCC	CTCTGAGGGCTGACACAAGG
MCP-1	CAACTCTCACTGAAGCCAGCTC	TAGCTCTCCAGCCTACTCATTGG
MIP-1α	CTTCTCTGTACCATGACACTCTGC	ATTCAGTTCCAGGTCAGTGATGTAT
TNF-α	GAGAAAGTCAACCTCCTCTCTG	GAAGACTCCTCCCAGGTATATG

Table S2. Antibodies for immunoblotting.

Antibody	Source	Vendor	Catalog No.
anti-phospho-JNK	Mouse	Santa Cruz Biotechnology	sc-6254
anti-JNK	Rabbit	Santa Cruz Biotechnology	sc-571
anti-phospho-p38	Rabbit	Cell Signaling Technology	#4511
anti-p38	Rabbit	Cell Signaling Technology	#8690
anti-phospho-ERK	Rabbit	Cell Signaling Technology	#4370
anti-ERK	Rabbit	Cell Signaling Technology	#4695
anti-phospho-NF-κB p65	Rabbit	Cell Signaling Technology	#3033
anti-NF-κB p65	Rabbit	Cell Signaling Technology	#8242
anti-phospho-IKKα/β	Rabbit	Cell Signaling Technology	#2697
anti-IKKα	Mouse	Cell Signaling Technology	#11930
anti-IKKβ	Rabbit	Cell Signaling Technology	#8943
anti-phospho-IκBα	Rabbit	Cell Signaling Technology	#2859
anti-IκBα	Mouse	Cell Signaling Technology	#4814
anti-iNOS	Rabbit	Cell Signaling Technology	#13120
anti-COX2	Rabbit	Cell Signaling Technology	#12282
anti-SIRT3	Rabbit	Cell Signaling Technology	#5490
anti-PPARα	Rabbit	Santa Cruz Biotechnology	sc-9000
anti-PPARβ	Rabbit	Santa Cruz Biotechnology	sc-7197
anti-PPARγ	Rabbit	Santa Cruz Biotechnology	sc-7196
α-tubulin	Mouse	Santa Cruz Biotechnology	sc-8035
GAPDH	Rabbit	Santa Cruz Biotechnology	sc-25778
Histone H3	Rabbit	Santa Cruz Biotechnology	sc-10809

Table S3. Compounds isolated from the pericarps of *Garcinia mangostana*

No	Name	Safety dosage (μM)	Structure
1	garcinone E	1.25	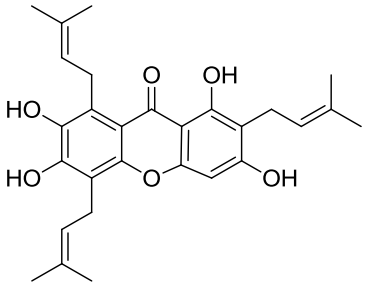
2	11-hydroxy-1-isomangostin	20	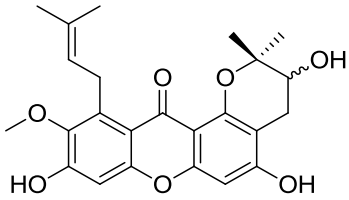
3	1,3,6,7-tetrahydroxy-8-prenylxanthone	20	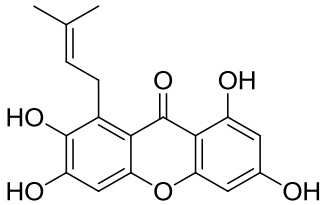
4	mangosharin	5	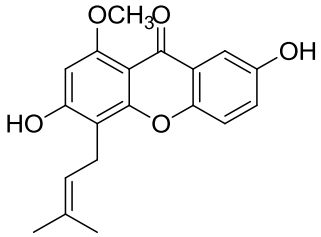
5	gartanin	2.5	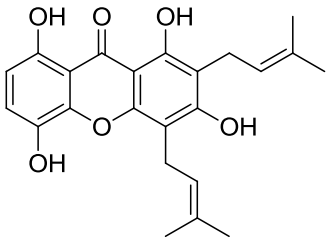
6	8-deoxygartanin	2.5	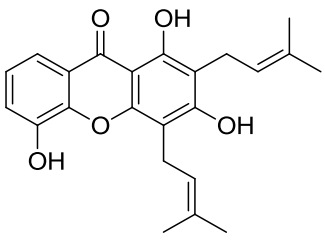

7	9-hydroxycalabaxanthone	2.5	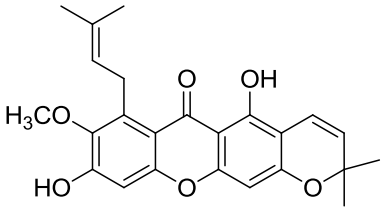
8	8-hydroxycudraxanthone G	5	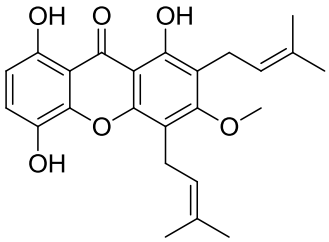
9	cudraxanthone G	10	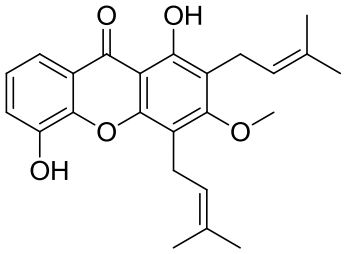
10	tovophylin A	2.5	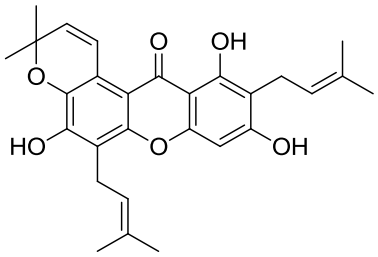
11	7-*O*-methylgarcinone E	5	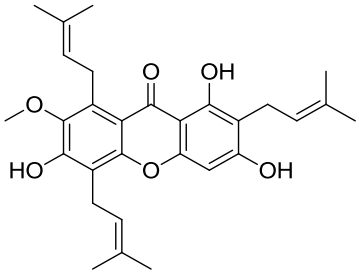
12	garcinone D	1.25	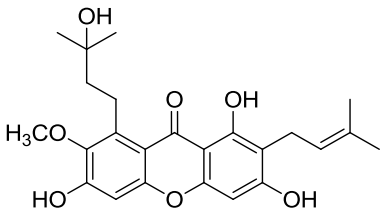

13	trapezifdixanthone	1.25	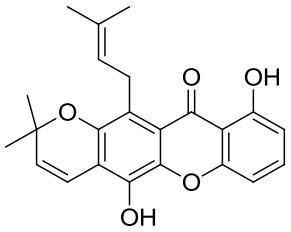
14	garcinone C	2.5	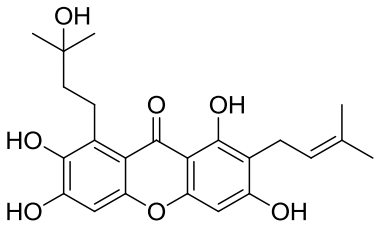

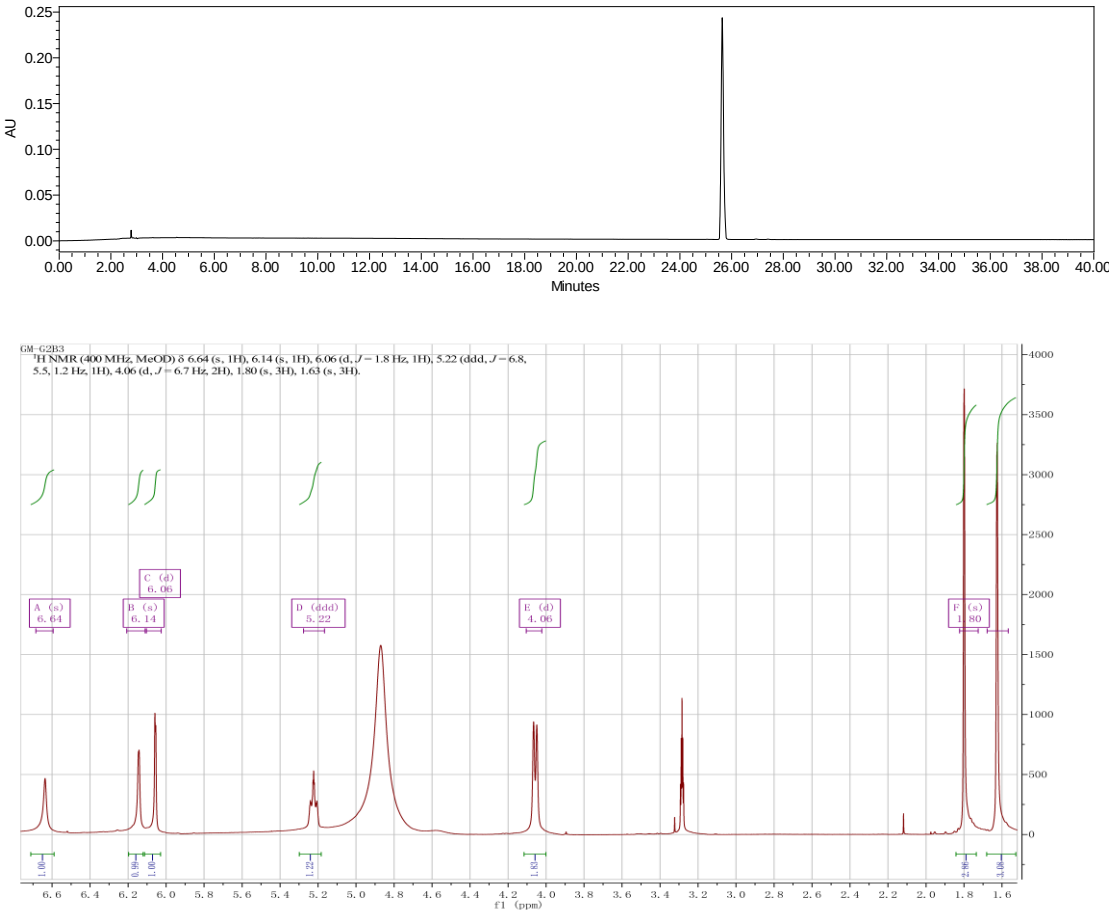

Figure S1. Top: The chemical profile of TPX analyzed by HPLC-UV. The accurately weighed TPX was dissolved in methanol (100 μg·mL) and sonicated for 1 h. After filtered by 0.45 μm Millipore membrane, 20 μL filtration was injected into an Agilent SB C18 column (250 × 4.6 mm, 5 μm) which was maintained at 35 ºC for gradient elution with water (A) and acetonitrile (B). The elution program was set as follows: 0-40 min, 95-0% A, 5-100% B. The detection wavelength was set at 254 nm. Representative chromatogram was analyzed using a Waters Empower system and the purity of TPX (99.8%) was determined by the peak area.

Bottom: ^{1}H NMR spectrum for TPX recorded in *d*6-DMSO. NMR spectrum was recorded on an ASCEND 600 MHz/54 mm NMR spectrometer. The chemical shift (δ) values are given in ppm with tetramethylsilane as internal standard, and coupling constants (J) are in Hz.

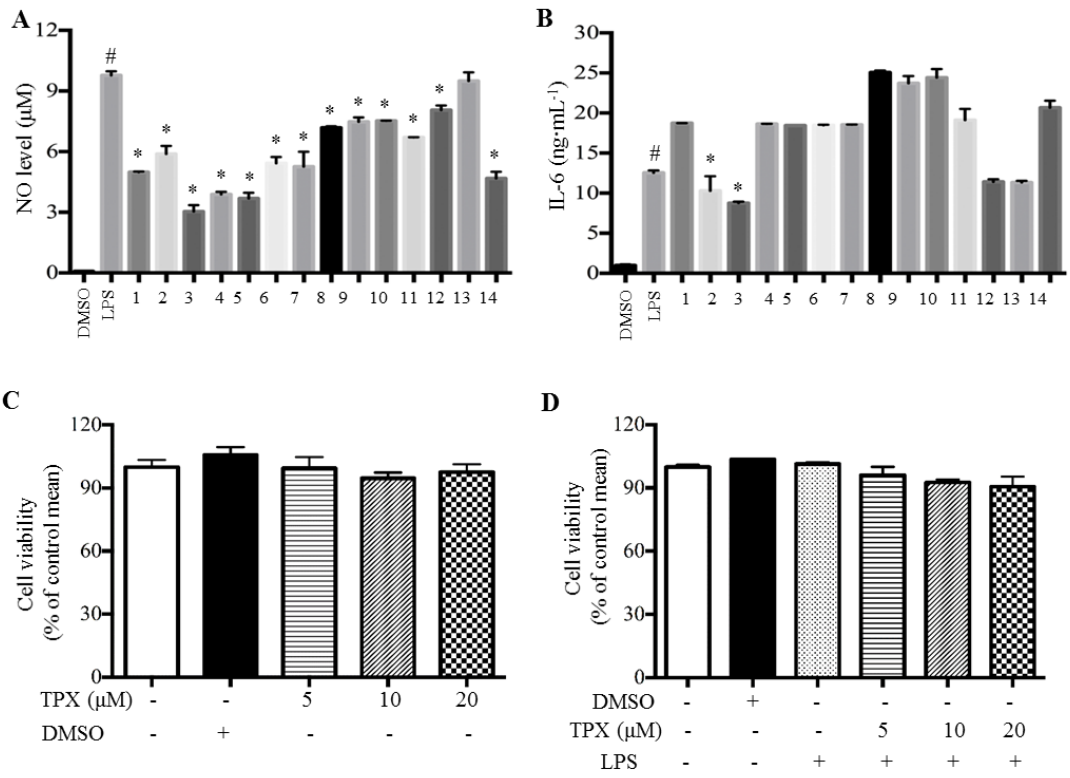

Figure S2. Screening of xanthones in LPS stimulated RAW264.7 cells. Cells were treated with different compounds from *G. mangostana*, ranging from 1.25 to 20 μM in the presence of LPS (1 μg·mL^{-1}). (A) NO production was determined using Griess reagent. (B) The levels of IL-6 were determined by ELISA kit. (C, D) The cytotoxicity of TPX on RAW264.7 cells with or without LPS. RAW264.7 cells were treated with TPX ranging from 5 to 20 μM in the presence or absence of LPS (1 μg·mL^{-1}) for 24h. Cell viability was determined by MTT assay. Data are normalized to the mean value of control group. **1**, 1.25 μM; **2**, 20 μM; **3**, 20 μM; **4**, 5 μM; **5**, 5 μM; **6**, 2.5 μM; **7**, 2.5 μM; **8**, 5 μM; **9**, 10 μM; **10**, 2.5 μM; **11**, 5 μM; **12**, 1.25 μM; **13**, 1.25 μM; **14**, 2.5 μM. Data are expressed as means ± SEM (n = 9). $^{\#}P < 0.05$ vs. DMSO, $^{*}P < 0.05$ vs. LPS.

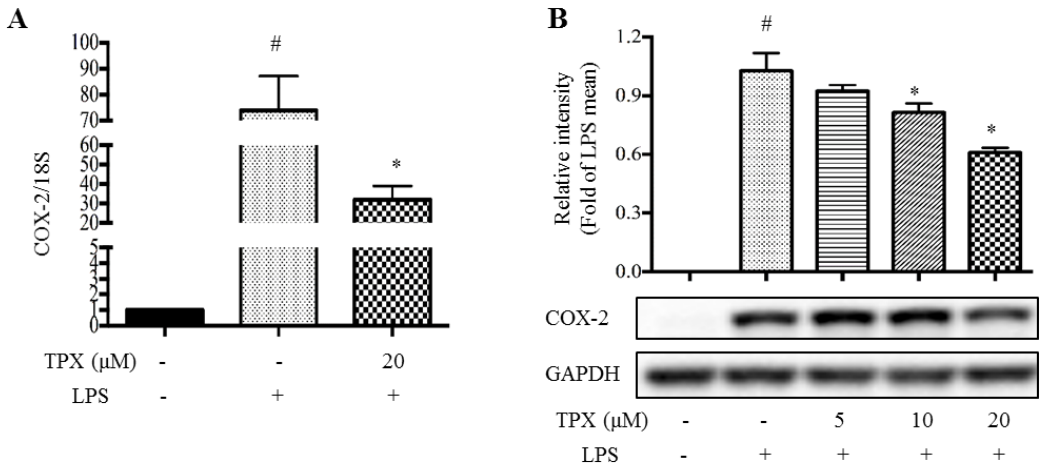

Figure S3. TPX inhibited LPS-induced COX-2 expression in RAW264.7 cells. (A) Cells were pretreated with the vehicle or TPX (20 μM) for 1h before treatment with LPS (1 μg·mL^{-1}) for 6h. The mRNA levels of COX-2 were analyzed by real-time qRT-PCR, normalized by 18S. (B) The protein level COX-2 was detected by Western blot analysis. Data are normalized to the mean value of LPS group. GAPDH was used as an internal loading control. Data are expressed as means ± SEM (n = 6). $^{\#}P < 0.05$ vs. DMSO, $^{*}P < 0.05$ vs. LPS.

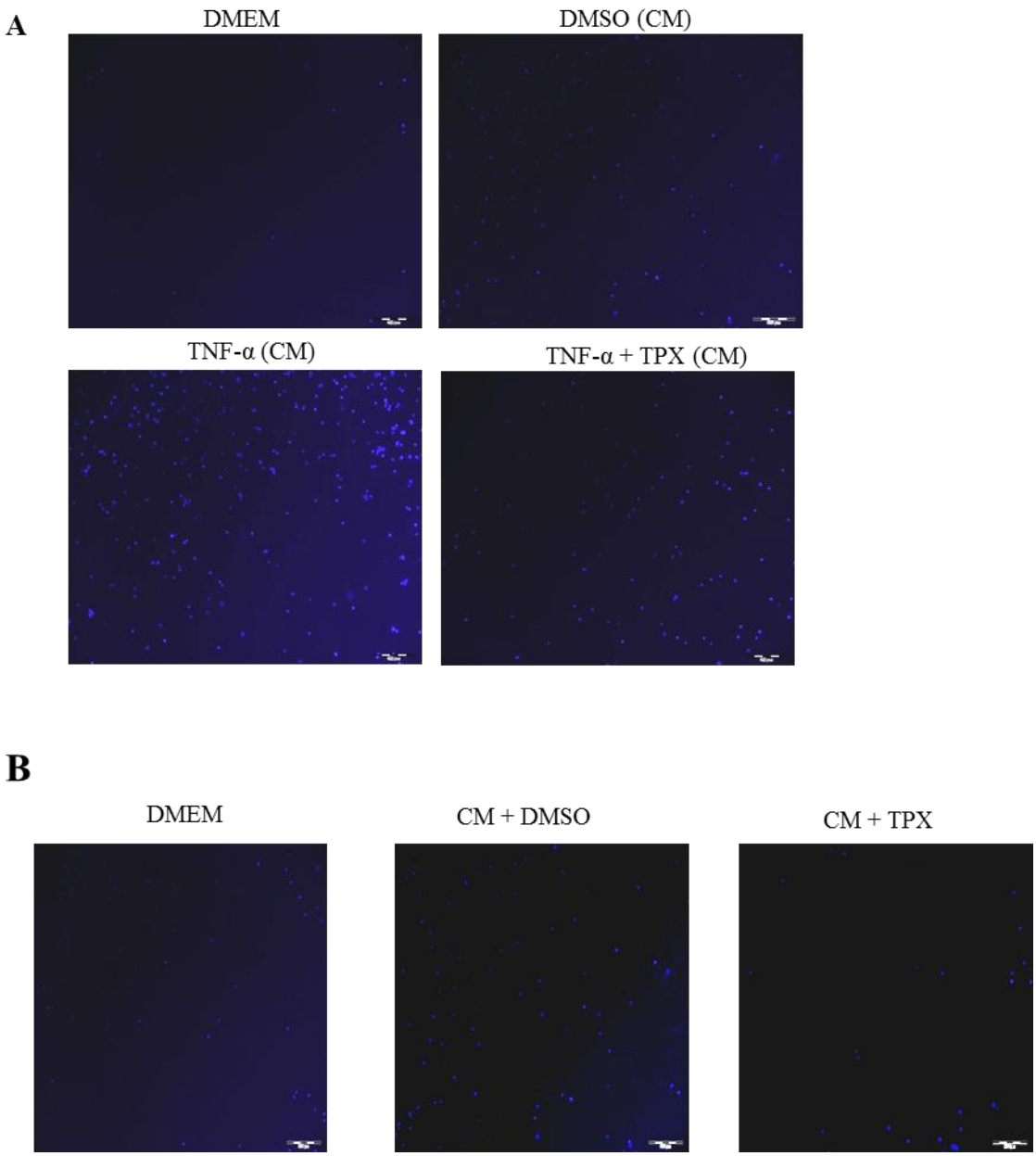

Figure S4. Transwell assay of macrophage migration. (A) Representative images of migrated macrophages in Figure 5A. (B) Representative images of migrated macrophages in Figure 5B.

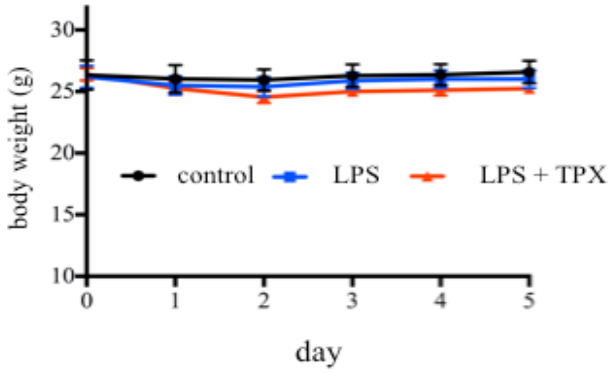

Figure S5. Effects of TPX on body weight in LPS-treated mice. Data are expressed as means ± SEM (*n* = 7).

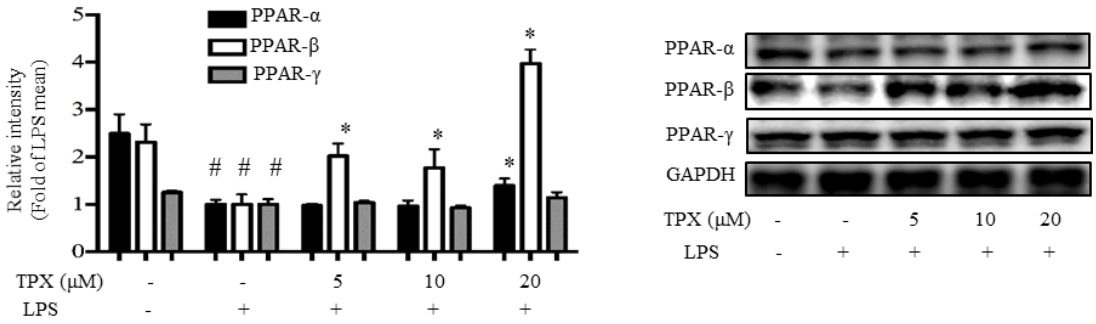

Figure S6. The protein expressions of PPARs were determined by Western blotting and GAPDH was used as an internal loading control. Data are normalized to the mean value of LPS group. Data are expressed as means ± SEM (n =5). $^{\#}P < 0.05$ vs. DMSO, $^{*}P < 0.05$ vs. LPS.

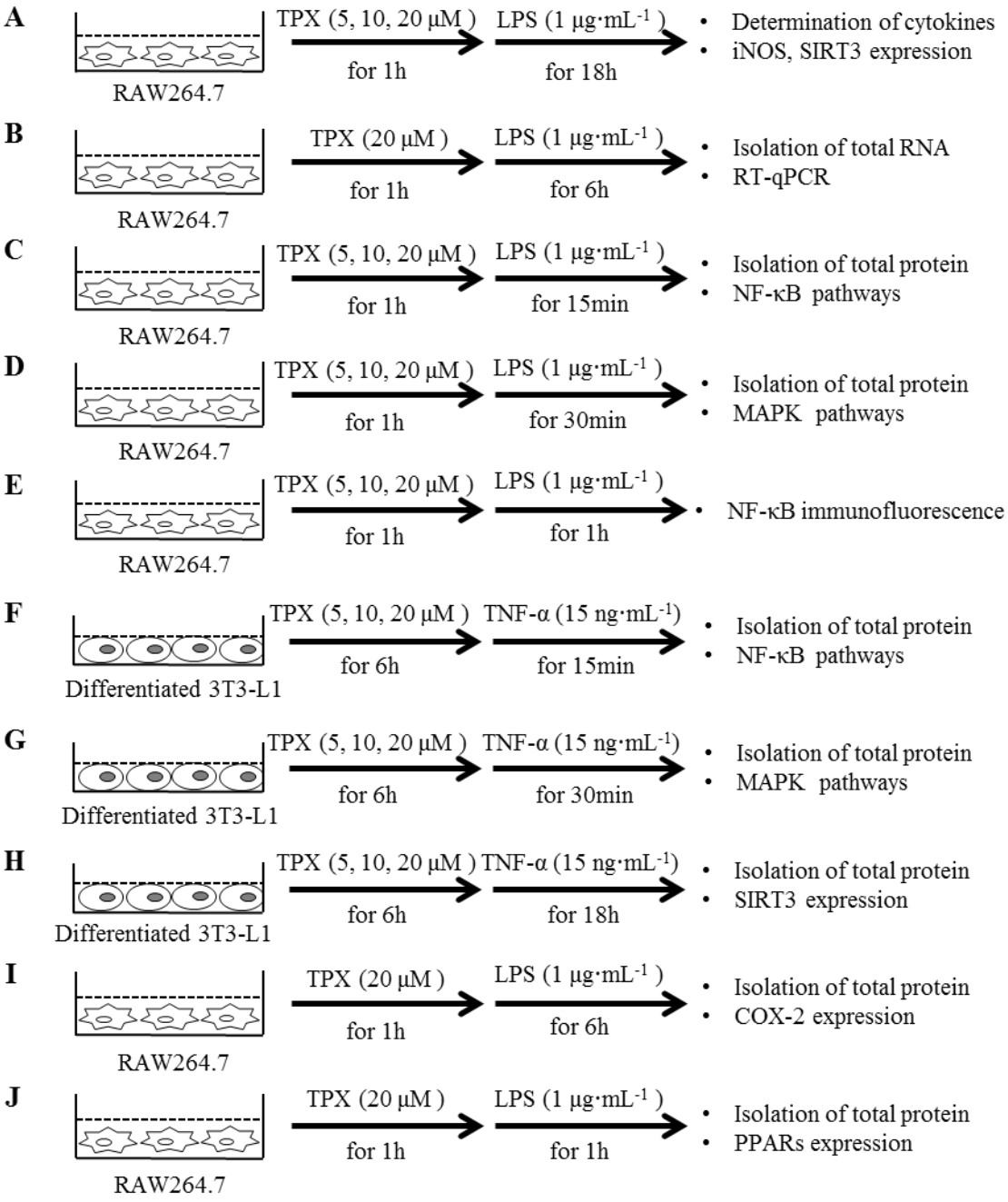

Figure S7. Schematic diagram of the *in vitro* experimental designs.